© 2015

PROCESSES OF CONVERSION OF A HOT METAL PARTICLE INTO AEROGEL THROUGH CLUSTERS

B. M. Smirnov[*]

Joint Institute for High Temperatures, Russian Academy of Sciences
127412, Moscow, Russia

Processes are considered for conversion into a fractal structure of a hot metal micron-size particle that is located in a buffer gas or a gas flow and is heated by an external electric or electromagnetic source or by a plasma. The parameter of this heating is the particle temperature, which is the same in all of the particle volume because of its small size and high conductivity. Three processes determine the particle heat balance: particle radiation, evaporation of metal atoms from the particle surface, and heat transport to the surrounding gas due to its thermal conductivity. The particle heat balance is analyzed based on these processes, which are analogous to those for bulk metals with the small particle size and its high temperature taken into account. Outside the particle, where the gas temperature is lower than on its surface, the formed metal vapor in a buffer gas flow is converted into clusters. Clusters grow as a result of coagulation, until they become liquid, and then clusters form fractal aggregates if they are removed form the gas flow. Subsequently, association of fractal aggregates join into a fractal structure. The rate of this process increases in middle electric fields, and the formed fractal structure has features of aerogels and fractal fibers. As a result of a chain of the above processes, a porous metal film may be manufactured for use as a filter or catalyst for gas flows.

1. INTRODUCTION

The behavior of a hot micron-size metal particle located in a gas or gas flow is of interest for various physical problems. Metals consisting of atoms with s and d electron shells are used widely as catalysts [1–4], which work due to electron transitions between s and d electron shells [5]. Catalytic properties may be stronger for metal clusters, and metal clusters as catalysts may be free [6, 7] or be attached to some oxide surfaces [8–11]. This is the basis of nanocatalysis [5, 12]. A hot metal particle in a plasma determines the character of plasmachemical processes [13–15]. In addition, the process of vaporization of a heated metal microparticle may be used for generation of metal clusters [16]. Hence, the behavior of a hot metal particle in a buffer gas is of interest for various problems.

In analyzing the processes involving a hot particle in a buffer gas, we consider two aspects below. The first group of processes determines a thermal equilibrium of the particle at a given power absorbed by the particle from an external source. Such a source may be gas discharge supported by constant or alternating electric fields, or it can emit electromagnetic waves of various wavelengths, including laser radiation. Because thermal equilibrium quickly sets in the particle due to its small size and high conductivity, we can characterize the action of an external energy source by the particle temperature, which is the same for all particle points. Processes that are responsible for particle heating include thermal radiation of the particle, heat transport from the particle to the buffer gas, and particle vaporization. The subsequent group of processes includes the evolution of a metal vapor resulting from particle vaporization. First, this atomic vapor is transformed into a gas of clusters in a gas flow, and subsequently these clusters grow as a result of coagulation and coalescence. When the temperature of the gas where metal clusters are located decreases below the melting point, association of clusters leads to the formation of fractal aggregates. In turn, they may join subsequently in other structures, in aerogels, or in fractal fibers if the growth process occurs in an external electric field.

In analyzing the character of processes with the participation of a metal particle located in a gas flow, we

---

[*]E-mail: bmsmirnov@gmail.com

3*
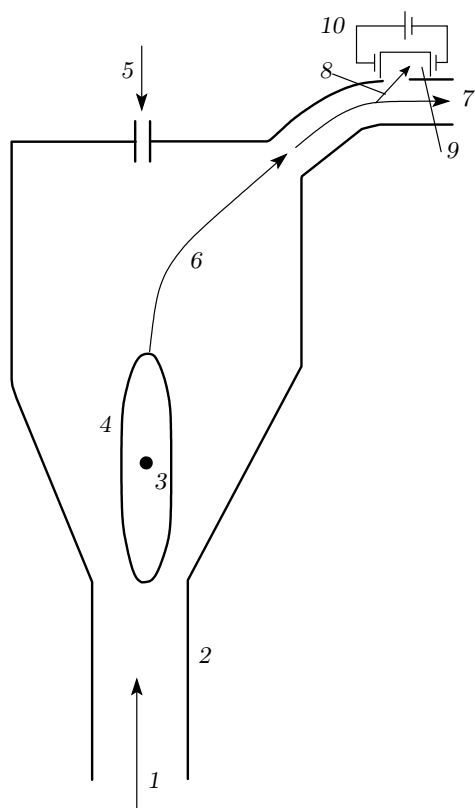
Fig. 1. Scheme of transformation of a heating metal microparticle in an argon flow in the course of generation of metal clusters and cluster structures: *1* — argon flow; *2* — aggregation chamber; *3* — microparticle; *4* — region of energy insertion from an external source; *5* — injection of microparticles in argon flow; *6* — line of flow propagation; *7* — yield gas flow; *8* — motion of clusters; *9* — region of growth of fractal structures; *10* — electric field

keep the scheme presented in Fig. 1 [14, 16]. In this scheme, a metal particle (or particles) drops (drop) in a flow of a gas and is heated by gas discharge plasma or electromagnetic radiation including the plasma formed under the action of this radiation. We do not consider this aspect of particle heating below, and characterize the degree of particle heating by the particle temperature. In addition, we restrict ourselves in some calculations by particles consisting of iron, copper, and silver; we are guided by a particle radius of 100 μm as a typical size of particles in production, and by argon as a buffer gas.

2. PROPERTIES OF HOT METAL PARTICLES AND METAL VAPORS

In considering the processes involving a hot metal particle in a buffer gas, we first prove the quiet char-

acter of the buffer gas flow. In Fig. 2, we show the Reynolds number Re of the particle in an argon flux in accordance with the formula [17]

$$\mathrm{Re} = \frac{vr}{\nu}, \qquad (2.1)$$

where $r = 0.1$ mm is the particle radius, ν is the argon viscosity at a given temperature, and v is the flow velocity. Because of small Reynolds numbers, motion of the flow has a laminar character. We take the velocity v_f of the vertical argon flow such that the Stokes force for particle interaction with the flow is equalized by the particle weight, and the particle is suspended in space. This velocity is given by [17]

$$v_f = \frac{2g\rho r^2}{9\eta}, \qquad (2.2)$$

where $g = 980$ cm/s^2 is the free fall acceleration, ρ is the particle density, and η is the argon viscosity.

Table 1 contains numerical parameters of metals and metal clusters [18–21] that are used in the analysis of processes in a buffer gas. The Wigner–Seits radius r_W is defined according to the relation [22, 23]

$$n = \left(\frac{r}{r_W}\right)^3, \qquad (2.3)$$

where n is the number of atoms for a particle of radius r. Values of the numbers of particle atoms n are given
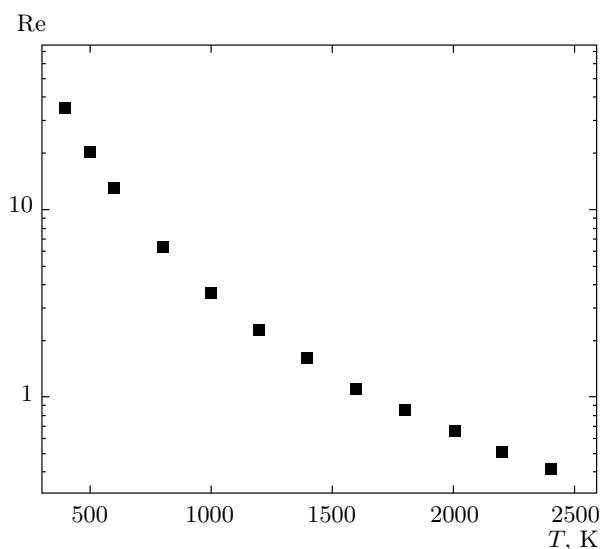
Fig. 2. The Reynolds number of a metal particle located in an argon flow at the velocity such that the particle weight equalizes the Stokes force. A particle radius is 0.1 mm, pressure is 0.1 atm

Table 1.   Some parameters of metals and metal vapors

Parameter	Fe	Cu	Ag
r_W, Å	1.47	1.47	1.66
n, 10^{17}	3.2	3.2	2.2
ε_0, eV	3.83	3.40	2.87
A, eV	3.0	2.2	2.0
E, J	0.14	0.17	0.12
Σ_0, 10^{17} s^{-1}	3.0	2.2	2.0
k	1.78	1.14	1.13
p_0, 10^6 atm	1.1	1.5	1.5
T_m, K	1812	1358	1235
T_b, K	3023	2835	2435

in Table 1 for the particle radius $r = 0.1$ mm. The total binding energy of atoms in a cluster consisting of n atoms is given by [24]

$$E = \varepsilon_0 n - An^{2/3}, \qquad (2.4)$$

and includes the first two terms in the expansion of this quantity over a small parameter $n^{-1/3}$. Here, ε_0 is the atom binding energy for a macroscopic particle, the parameter A characterizes the surface cluster energy, and the values of these parameters are presented in Table 1 for metals under consideration together with the total binding energy E of particle atoms.

We take the temperature dependence of the metal conductivity Σ in the form

$$\Sigma = \Sigma_0 \left(\frac{300}{T} \right)^k. \qquad (2.5)$$

The parameters of this formula are given in Table 1 for the relevant metals. In addition, the saturation vapor pressure p_{sat} is approximated by the formula

$$p_{sat} = p_0 \exp \left(-\frac{\varepsilon_0}{T} \right). \qquad (2.6)$$

Parameters of metals and their clusters given in Table 1 are used below. In this consideration, we assume the cluster temperature T to be the same at all points of the particle volume. Using values of the metal conductivity, we can estimate a typical time of establishment of the identical temperature over the particle volume; this time is less than 10^{-8} s. Times of processes under consideration significantly exceed this value. Table 1 also contains values of the melting point T_m and the boiling point T_b for metals under consideration. We note that the particle temperature lies in the range between the melting and boiling points.

3. PROCESSES OF HEAT BALANCE OF A HOT METAL PARTICLE

Taking the particle temperature as a parameter that determines the degree of its excitation, we find the power P that is absorbed by a hot metal particle and support a given temperature. The heat balance equation in this case has the form

$$P = P_{rad} + P_{ev} + Q, \qquad (3.1)$$

where P_{rad} is the radiation power emitted by the particle, P_{ev} is the power consumed on evaporation of atoms, and the power Q is determined by heat transport to the buffer gas via its thermal conductivity. A hot particle emits radiation from a skin layer near its surface, and the depth of the skin layer is of the order of photon wavelengths. The problem of absorption and scattering of electromagnetic radiation by a planar metal surface is solved in detail in book [25]. In the case under consideration, a radiating surface can be reduced to a planar surface, and based on the detailed balance principle, we obtain the grey coefficient $a(\omega)$ of the metal surface for a given frequency ω in the form [25]

$$a(\omega) = \sqrt{\frac{\alpha}{2}} \left[\ln \left(\frac{1}{\alpha} \right) - \frac{\pi}{2} + 1 \right],$$
$$\alpha = \frac{\omega}{4\pi\Sigma} \ll 1. \qquad (3.2)$$

The smallness of the grey coefficient $a(\omega)$ is determined by the high metal conductivity, which leads to a small parameter α. This gives the radiation power emitted by the particle

$$P_{rad} = a(T) \cdot 4\pi r^2 \sigma T^4, \qquad (3.3)$$

where σ is the Stephan–Boltzmann constant and $a(T)$ is the grey coefficient averaged over frequencies. Practically, averaging reduces to using the grey coefficient at the radiation wavelength λ related to the maximum radiation power at a given temperature in accordance with the Wien law [26], $\lambda = 0.30$ cm $\cdot$ K$/T$, where the particle temperature T is expressed in K.

Instead of the particle temperature, it is convenient to use its reduced value

$$x = \frac{T}{2000}. \qquad (3.4)$$

Using this parameter, we can approximate the grey coefficient for the surface of pure metals as

$$a = a_0 x^{k_r}. \qquad (3.5)$$
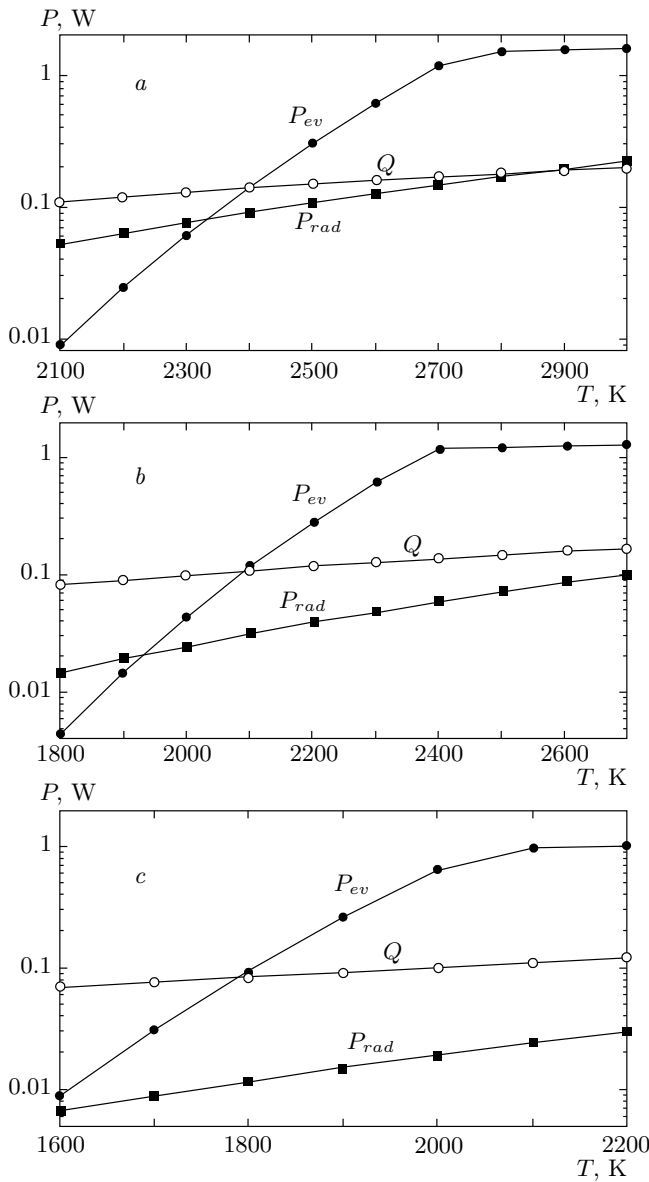
Fig. 3. Heat balance of a metal particle of a radius of 0.1 mm heated by an external source. The particle material is (*a*) Fe, (*b*) Cu, and (*c*) Ag

Table 2. Parameters of the heat balance for a metal particle located in a buffer gas

Parameter	Fe	Cu	Ag
a_0	0.37	0.22	0.17
k_r	0.1	0.75	0.70
P_0, W/mm^2	4.2	2.5	1.9
k_1	4.13	4.73	4.67
D_0, cm^2/s	43	42	33
ν_1, 10^{28} $(cm \cdot s)^{-1}$	2.2	2.9	2.3
P_1, 10^9 W/cm	1.3	1.6	1.0
ε	22.2	19.7	16.6
ν_2, 10^{20} s^{-1}	2.0	1.9	1.5
P_2, W/cm	120	105	70
T_*, K	2740	2690	2020
$D(T_*)$, cm^2/s	74	70	33
T_ξ, K	2400	2100	1800

Values of parameters in this formula are given in Table 2. Accordingly, the radiation power P_{rad} emitted by the particle takes the form

$$P_{rad} = P_0 r^2 x^{k_1}, \qquad (3.6)$$

where r is the particle radius, and the parameters of this formula are contained in Table 2 for metals under consideration. In addition, Fig. 3 gives the dependence $P_{rad}(T)$ for metal particles under consideration.

The power consumed on atom evaporation from the particle surface is equal to $P_{ev} = \nu_{ev}\varepsilon_0$, where ν_{ev} is the rate of evaporated atoms from the particle surface and ε_0 is the atom binding energy for this metal. There are two mechanisms of atom evaporation from the particle surface. In the first case, the number density N_a of buffer gas atoms significantly exceeds the number density $N_{sat}(T)$ of metal atoms that corresponds to the saturated vapor pressure for this metal at a given temperature. Then the number density of metal atoms at the particle surface is equal to the saturated number density N_{sat}, and equilibrium near the surface leads to the equality of fluxes of evaporated and attached atoms, whereas the resultant flux of evaporated atoms from the particle surface is less than each of these values and is determined by diffusion of metal atoms in the buffer gas due to a gradient of the concentration of metal atoms in the buffer gas. Ignoring the influence of motion of the buffer gas on the character of atom removal from the particle surface, we express the rate of atom evaporation from the particle surface in this regime according to the Smolukhowski formula as [27]

$$\nu_{ev} = 4\pi r D_m N_{sat}(T), \qquad (3.7)$$

where r is the particle radius and D_m is the diffusion coefficient of metal atoms in the buffer gas. Taking the temperature dependence of the diffusion coefficient in the form

$$D_m = D_0 x^\beta, \qquad (3.8)$$

where $\beta \approx 1.7$ [28], we give the parameters of this formula for argon as a buffer gas at the argon pressure

$p = 0.1$ atm in Table 2, based on [29]. Based on formula (2.6), we represent expressions for the rate ν_{ev} of atom evaporation from the particle surface and the power of evaporation P_{ev} in the form

$$\nu_{ev} = \nu_1 r x^{\kappa_1} \exp\left(-\frac{\varepsilon}{x}\right),$$
$$P_{ev} = P_1 r x^{\kappa_1} \exp\left(-\frac{\varepsilon}{x}\right). \tag{3.9}$$

The parameters of formula (3.9) are given in Table 2.

For another mechanism of particle vaporization, $N_a \ll N_{sat}(T)$, the evaporation rate is given by [19, 30]

$$\nu_{ev} = 4\pi r^2 \sqrt{\frac{T}{2\pi m}}\, N_{sat}(T), \tag{3.10}$$

where m is the mass of evaporated atoms. But the number density of atoms cannot exceed the value $N_a(T)$ that corresponds to a current gas pressure and is established for a time $t \sim r/c_s$, where c_s is the sound speed at the particle temperature; for the conditions under consideration, $t \sim 10^{-7}$ s. Therefore, at temperatures where $N_{sat}(T) \geq N_a$, the number density of metal atoms near the surface is $N_m = N_a$, and the atom evaporation rate by analogy with formula (3.9) is equal to

$$\nu_{ev} = 4\pi r D_m N_a(T). \tag{3.11}$$

Correspondingly, using the analogy with formula (3.10), we obtain the following expressions for the rate ν_{ev} of atom evaporation and for the evaporation power P_{ev}:

$$\nu_{ev} = \nu_2 r x^{\kappa_1}, \quad P_{ev} = P_2 r x^{\kappa_1}. \tag{3.12}$$

Table 2 gives the parameters of formula (3.12) along with the temperature T_* of transition between the above mechanisms of particle vaporization according to the relation

$$N_a = N_{sat}(T_*). \tag{3.13}$$

The parameters in Table 2 correspond to the argon pressure $p = 0.1$ atm. Figure 3 contains the temperature dependence for the power consumed on vaporization of metal particles of the radius 0.1 mm.

The evaporation rate allows us to determine the particle lifetime if this process occurs at a constant temperature. Indeed, the balance equation for a number n of particle atoms has the form

$$\frac{dn}{dt} = -\nu_{ev}, \tag{3.14}$$
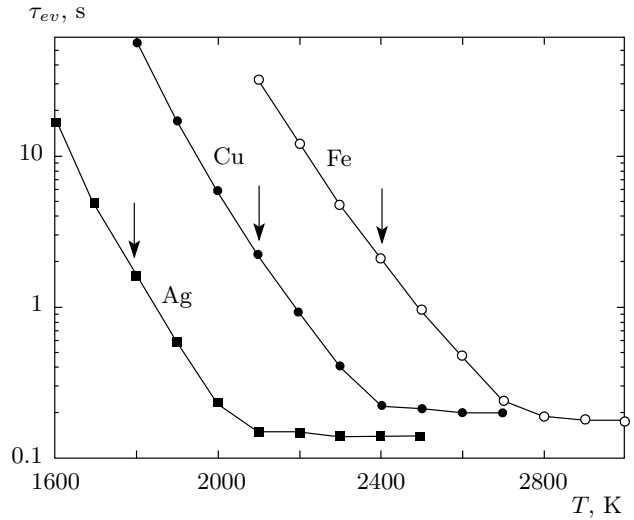
Fig. 4. Evaporation time (lifetime) for a metal particle of a radius of 0.1 mm as a function of temperature. Arrows indicate the temperatures T_ξ at which the efficiency of particle vaporization is one half

and because the evaporation rate ν_{ev} is proportional to the particle radius or $N^{1/3}$, the particle lifetime τ_{ev} follows from the solution of this equation and is given by

$$\tau_{ev} = \frac{3n_0}{2\nu_{ev}}, \tag{3.15}$$

where n_0 is the initial number of particle atoms. The temperature dependences for the total evaporation time of metal particles of a radius 0.1 mm are given in Fig. 4.

Because of small Reynolds numbers, according to Fig. 2, convection of a gas flow near the particle is absent, and heat transport to the buffer gas is determined by the gas thermal conductivity. We use the following temperature dependences for the thermal conductivity $\kappa(T)$ and the thermal diffusion $\chi(T)$ coefficients of argon [29, 31]:

$$\kappa(T) = \kappa_0 \left(\frac{T}{1000}\right)^{0.68},$$
$$\chi(T) = \chi_0 \left(\frac{T}{1000}\right)^{1.68}, \tag{3.16}$$

where $\kappa_0 = 4.2 \cdot 10^{-4}$ W/cm $\cdot$ K and $\chi_0 = 38$ cm^2/s at the argon pressure $p_0 = 0.1$ atm. The power Q that is scattered as a result of heat transport from the particle

P, W
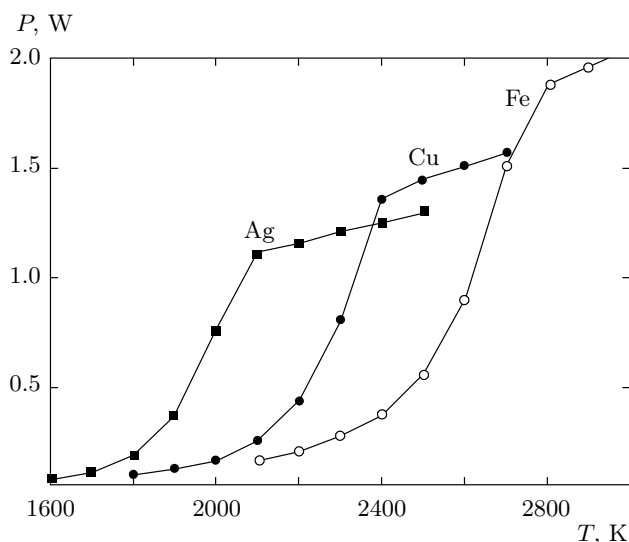
Fig. 5. Total power scattered by a heated metal particles of a radius of 0.1 mm

to argon is

$$Q = 4\pi R^2 \kappa(T)\frac{dT}{dR} = 4\pi r T_0 \kappa(T_0) \left(\frac{T}{1000}\right)^{1.68} =$$
$$= Q_0 r x^{1.68}, \quad (3.17)$$

where T and R are the current temperature and the distance from the particle center, and T_0 and r are the temperature on the particle surface and its radius. Since the parameter $Q_0 = 10$ W/cm in formula (3.17) describes heat transport in argon, it is the same for all metals under consideration. Figure 3 gives the partial powers for a metal particle of a radius of 0.1 mm located in an argon flow, with the power of particle radiation given by formula (3.7), the power of evaporation taken in accordance with formulas (3.9) and (3.12), and the power of heat transport in argon given by formula (3.17).

The results in Fig. 3a relate to iron, Fig. 3b describes data for copper, and Fig. 3c contains results for silver. In addition, Fig. 5 gives the total powers that are scattered by metal particles heated up to a given temperature in accordance with formula (3.1). We can introduce the efficiency ξ of particle evaporation as a result of particle heating, i. e., the ratio of the power consumed on evaporation of particle atoms to the total power of particle heating, according to the formula

$$\xi(T) = \frac{P_{ev}}{P}. \quad (3.18)$$

Table 2 contains the temperature T_ξ above which the efficiency of particle evaporation exceeds one half.
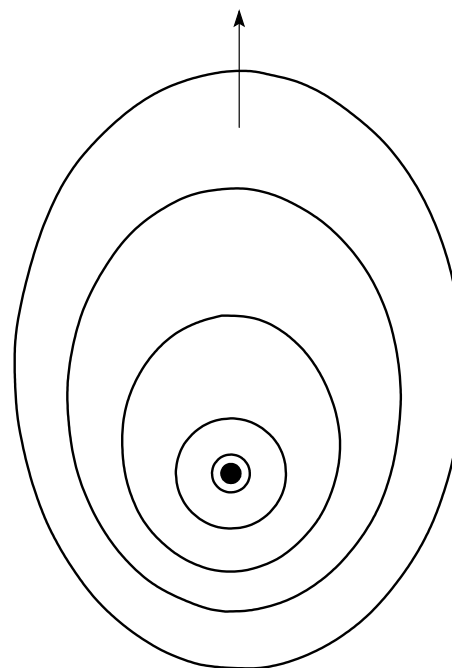
Fig. 6. Schematic form of lines of identical temperatures in the process of argon flow through a hot metal particle

The above consideration of the particle heat balance relates to a motionless particle, that is, the surface of identical temperatures are spheres whose centers coincide with the particle center. Figure 6 schematically gives the cross section of the surfaces of identical temperatures if a buffer gas flows around the particle. For the above consideration, the criterion is required that the spherical character of isothermal surfaces is violated far from the particle, which takes the form

$$R = \frac{\chi}{v} \gg r, \quad (3.19)$$

where v is the flow velocity. If the flow velocity is taken in accordance with formula (2.2), such that the Stokes force equalizes the particle weight, then we can obtain $R \approx 0.1$–1 cm, and hence criterion (3.19) holds true.

Thus, we obtain the following behavior pattern for a metal micron-size particle heated by an external source in an argon flow. The heat balance of this particle consists in the evaporation of atoms from the particle surface and heat transport to the surrounding argon, while particle radiation makes a small contribution to the heat balance because of a small particle size. Argon stream motion is not essential near the particle, where heat transport is similar to that of a motionless particle. Below, we use this understanding of particle behavior for the analysis of nucleation processes.

4. CLUSTER GROWTH FROM EVAPORATING METAL ATOMS

The metal vapor formed as a result of vaporization of a hot metal particle is captured by a gas flow outside the particle and travels in a region of lower temperatures, where the partial pressure of this vapor exceeds the saturated vapor pressure at a current flow temperature and metal atoms are transformed into clusters. As a result, a vapor excess is converted into clusters, and the nucleation process occurs in two stages. In the first stage, metal atoms are transformed into clusters, and in the second stage, cluster growth results from coagulation and coalescence until the clusters become solid. We consider the first stage where growth of metal clusters proceeds according to the scheme [32]

$$A + 2M \rightarrow A + M_2, \quad M_n + M \rightarrow M_{n+1}. \quad (4.1)$$
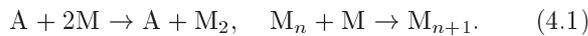
Here, A is a buffer gas atom, M is a metal atom, and the index indicates the number of cluster atoms. The first process is slow as a three-body process, and buffer gas atoms carry an excess of energy that is released as a result of formation of a bond between colliding metal atoms. In attachment of atoms to molecules and clusters, this excess energy goes to vibration degrees of freedom for a forming particle and subsequently this energy transfers to buffer gas atoms collided with a growing cluster.

In this scheme, the process of formation of condensation nuclei is a three-body process, i. e., a slow process compared with the attachment process of free metal atoms to clusters. As a result, small clusters are practically absent in the size distribution function, and this process is governed by the large parameter [32]

$$G = \frac{k_0}{K N_a} \gg 1, \quad (4.2)$$

where k_0 is the reduced rate constant for atom–cluster collisions, K is the rate constant of the three-body process, and N_a is the number density of buffer gas atoms. The values of the reduced rate constant k_0 at temperature 1000 K are given in Table 3 according to [16], and its basic temperature dependence is $k_0 \propto \sqrt{T}$. The rate constant of the three-body process can be estimated by an order of magnitude as $K \sim 10^{-33}$–10^{-32} cm^6/s, and on the basis of experimental data, we take it as $K = 3 \cdot 10^{-33}$ cm^6/s. From this, we can estimate $G \approx$ $\approx 5 \cdot 10^4$ K at temperature $T = 2000$ K for metals under consideration. If we assume the buffer gas with metal atoms to be a uniform matter, and its temperature to be constant during this process, then we obtain the average number $\overline{n}$ of cluster atoms at the end of

Table 3.   Parameters of cluster growth

—	Fe	Cu	Ag
k_0, 10^{-11} cm^3/s	2.1	2.7	3.0
$G(T_0)$, 10^4 K	8.5	5.5	4.4
$\overline{n}_0$, 10^3	6.0	4.3	3.6
τ_{cl}, 10^{-5} s	9.7	7.6	7.5
T_ξ, K	2400	2100	1800
P_ξ, W	0.28	0.24	0.18
v_ξ, m/s	1.5	1.9	2.4
$N_{sat}(T_\xi)$, 10^{16} cm^{-3}	3.1	3.7	6.0
t_m, s	0.01	0.015	0.014
$\overline{n}$, 10^5	2.4	4.1	13
N_{cl}, 10^{11} cm^{-3}	1.3	0.91	0.51
R_m, cm	2.0	2.0	1.7
r, nm	9.2	11	16
n_a, 10^3	4.0	3.0	1.3
ρ_a, g/cm^3	0.06	0.09	0.15
V_f, mm^3	0.45	0.38	0.26

this process of vapor conversion in a gas of clusters and the time τ_{cl} of this process as [19, 21]

$$\overline{n} = 1.2 G^{3/4}, \quad \tau_{cl} = \frac{3.2 G^{1/4}}{N_m k_0}, \quad (4.3)$$

where N_m is the number density of metal atoms. Table 3 contains the parameters of this formula under the assumption that this process of conversion of atom vapor into clusters proceeds at the temperature T_ξ. In addition, we can estimate a typical time τ_{th} of heat transition from the particle to the gas flow, which, according to formula (3.19), is equal to

$$\tau_{th} \sim \frac{R^2}{\chi} \sim \frac{\chi}{v^2}, \quad (4.4)$$

and for a typical flow speed $v \sim 2$ m/s, we can estimate a typical time of heat transport as $\tau_{th} \sim 10^{-3}$ s.

Thus, because of a high density of metal vapor, a typical time of conversion of metal atoms into clusters at an appropriate temperature is small compared with the cooling time. Therefore, formation of metal clusters proceeds adiabatically with conservation of the equilibrium between the number density N_m of free metal atoms and clusters, which is given by [19, 21]

$$N_m = N_{sat}(T) \exp\left(-\frac{A}{T n^{1/3}}\right). \quad (4.5)$$

Here, n is the average number of cluster atoms, and under typical conditions, the second term in the right-hand side of (4.5) is unity. When liquid clusters are formed, their subsequent growth is determined by co-agulation only. Then the average number $\overline{n}$ of cluster atoms is given by [19, 21]

$$\overline{n} = 6.3(N_b k_0 t)^{1.2}, \qquad (4.6)$$

where N_b is the total number density of cluster atoms and t is the time of the coagulation process. Coagulation of liquid clusters proceeds simultaneously with the cooling of the flow and finishes when the buffer gas temperature reaches the metal melting point, which practically coincides with the melting point of clusters because of their large size.

We find typical times of the above processes assuming that optimum conditions correspond to the particle temperature T_ξ, where evaporation of particle atoms and heat transport to surrounding argon due to thermal conductivity give an identical contribution to the power scattered by a hot particle. Table 3 contains this temperature and the total power P_ξ to support this particle temperature and the flow velocity v_ξ in accordance with formula (2.2), where the particle weight is equalized by the Stokes force, such that the particle hangs in space. We note that conversion of atom vapor into clusters according to equilibrium (4.5) proceeds at temperatures at which the partial vapor pressure is much lower than the saturated vapor pressure. According to formula (2.6), that pressure decreases by e times if the temperature decreases by the value $\delta T \sim T^2/\varepsilon_0 \sim 100$ K, i. e., variation of the temperature for the start of metal condensation is relatively small. This means that formation of clusters occurs in the region, which may be considered as a motionless one.

Because the argon flow transfers the heat scattered by the particle through nucleation of evaporated atoms and heat transport owing to thermal conductivity, we obtain the heat balance equation in the form

$$P_\chi = c_p (T - T_0) S v, \qquad (4.7)$$

where $c_p = 5/2$ is the heat capacity per atom, T_0 is the temperature of the surrounding argon, which we take as $T_0 = 300$ K, $S = \pi R^2$ is the flow cross section, and v is the flow speed, which we take to be v_ξ for simplicity. This gives $R \approx 2$ cm in all cases, and the time of heat transfer to the flow is approximately 8 ms for all cases as well. A typical time of formation of the flow with the melting point T_m for these metals is t_m, the number density N_b of bound atoms at that time coincides with the number density N_{sat} at saturated vapor pressure at the particle temperature T_χ, the average number $\overline{n}$ of cluster atoms at its transition in the solid state is determined by formula (4.6) at that time, r is the cluster radius that corresponds to its size in accordance with formula (2.3), and R_m is the flow radius at this time. The values of these parameters are given in Table 3.

The joining of solid clusters results from cluster contacts, which leads to formation and growth the fractal aggregates. We are guided by the model of diffusion-limited aggregation [33] with the diffusion character of cluster motion, which leads to the fractal dimension $D = 1.77$ of the forming fractal aggregate; this value is confirmed by measurements [34, 35]. Then the number n_a of elemental monomers of a radius a, i. e., the number of solid clusters in some fractal aggregate of a radius R, is given by

$$n_a = \left(\frac{R}{a}\right)^D. \qquad (4.8)$$

As the aggregate size increases, its density decreases, as does their stability due to thermal fluctuations [36]. Usually, the maximum aggregate size is restricted by $R \sim 1$ μm, and for definiteness we take the aggregate maximum radius to be $R = 1$ μm. Table 3 contains the number of monomers n_a in one aggregate in accordance with formula (4.8). The rate of this process in the diffusion regime of aggregation is given by [18]

$$\frac{dn_a}{dt} = \frac{1}{2} k_{as} N_{cl}, \qquad (4.9)$$

and the rate constant of association of aggregates at the temperature $T = 500$ K in argon is $k_{as} = 5.5 \cdot 10^{-10}$ cm^3/s. As a result, we can obtain the growth time of fractal aggregates up to the size $R = 1$ μm approximately as $\tau_a = 2$ min in all the metal cases. We can see that the growth of a fractal aggregate is a slow process, and its realization requires the removal of metal clusters from the gas flow.

The growth of fractal structures in an external electric field results from the interaction of associated aggregates via induced dipoles and leads to formation of fractal fibers [37, 38]. As a result, various structures with fractal properties may be formed [35, 39]. The rates of aggregation in an electric field and in the absence of external fields are equalized at the electric field strength E_* according to the relation [18]

$$E_*^2 \approx \frac{T}{a^5 N_a^{2/3}}, \qquad (4.10)$$

where N_a is the number density of aggregates of a radius a. This formula shows that the action of an electric

field is the stronger, the smaller is the size of an aggregate in the course of its growth. According to this formula, the electric field strength for the aggregate size $R = 1$ μm and for all metals under consideration is $E_* \approx 200$ V/cm. Action of the electric field leads to formation of fractal fibers [37, 38]: formed fractal structures are elongated along the field. Interwoven fractal fibres form a fractal tangle [39], and just this object is of interest as a rareness porous metal. Thus, a fractal structure is gathered now from individual fractal aggregates whose size a is given by formula (4.10) at a given electric field strength. If $R = 1$ μm, then the density ρ_a of a formed structure for metals under consideration is given in Table 3, together with the specific area S of internal surface. The first parameter coincides with that for aerogels [40, 41] by an order of magnitude, and the second is less than that for strongly porous materials. In addition, Table 3 contains the volume V_f of a fragment of this fractal structure that is formed from one metal particle of a radius of 0.1 mm.

We note one more aspect of these processes, which first occur in a buffer gas flow near a hot metal particle. The processes of cluster formation from evaporated metal atoms take place inside the flow for times when the flow propagates over small distances compared to the size of the aggregate chamber. The joining of two solid clusters lasts about 0.01 s and may proceed inside the flow. But the total time of formation of fractal structures takes minutes, and hence this process must occur outside the gas flow. For this goal, it is necessary to use impactors [42, 43] to separate particles from the flow. An example of this impactor is shown in Fig. 1. As a result, growth of fractal structures from solid clusters occurs in a quiet region with an electric field. One more remark relates to the number of particles that are heated simultaneously in the framework of the scheme in Fig. 1. In the case of several heated particles, it is necessary that the distance between neighboring particles exceed their size significantly, and the buffer gas flow to be able to transfer the released energy.

5. CONCLUSION

The above analysis of the processes in the course of conversion of an atomic vapor resulting from vaporization of a heated metal microparticle exhibits the possibility to obtain a rareness fractal structure consisting of nanometer solid clusters in the end of these processes. Fragments of this structure are fractal aggregates. The chain of processes under consideration includes fast processes involving metal atoms and their

clusters in the flow of a buffer gas, whereas processes of formation and growth of fractal structures proceed slowly and must be outside the buffer gas flow. Understanding the character of these processes is necessary for realizing the generation of a fractal structure that has features of an aerogel and fractal fibers.

The product of the processes under consideration, a fractal structure, is a rareness porous structure. Because fragments of this structure are fractal aggregates, it resembles an aerogel, and because these fragments are joined into a structure in an external electric field, this structure is akin to fractal fibers. Usually, metals consisting of atoms with nonfilled s and d electron shells are used as catalysts [1–3, 5]. Therefore, fractal structures resulting from processes under consideration are convenient catalysts for processes in gaseous mixtures contained in a flow through such a structure because of a high specific area of its internal surface. We note that it follows from the results of the above estimations that one metal microparticle of a radius 0.1 mm used in the estimations allows preparing a membrane of the depth of 10 cluster layers and of an area of the order of 1 mm^2. In addition, the above analysis gives algorithms for estimations related to other geometric schemes for manufacturing porous metal membranes and different metals. We can add to this that if two particles of different metals are injected in the region of excitation, a fractal structure of a metal alloy can be prepared.

REFERENCES

1. G. C. Bond, *Catalysis by Metals*, Acad. Press, London (1962).

2. M. Haruta, The Chemical Record **3**, 75 (2003).

3. G. C. Bond, C. Louis, and D. T. Thompson, *Catalysis by Gold*, World Sci., Singapore (2006).

4. K. W. Kolasinski, *Surface Science: Foundation of Catalysis and Nanoscience*, Wiley, Berlin (2012).

5. R. Coquet, K. L. Howard, and D. J. Willock, Chem. Soc. Rev. **37**, 2046 (2008).

6. K. Judai et al., J. Amer. Chem. Soc. **126**, 2732 (2004).

7. R. S. Berry and B. M. Smirnov, Phys. Rep. **527**, 205 (2013).

8. M. Haruta, Catal. Today **36**, 153 (1987).

9. M. Haruta, T. Kobayashi, H. Sato, and N. Yamada, Chem. Lett. **2**, 405 (1987).

10. G. C. Bond and D. J. Thompson, Catal. Rev. Sci. Eng. **41**, 319 (1999).

11. M. Chen and D. W. Goodman, Acc. Chem. Res. **39**, 739 (2006).

12. *Nanocatalysis*, ed. by U. Heiz and U. Landman, Wiley, Berlin (2007).

13. A. Klimov, V. Biturin, V. Chinnov et al., AIAA Paper **8**, 1323 (2011).

14. A. Klimov, V. Biturin, A. Grigorenko et al., AIAA Paper **8**, 3285 (2011).

15. P. V. Kashtanov, B. M. Smirnov, V. A. Biturin, and A. I. Klimov, Europhys. Lett. **96**, 33002 (2011).

16. B. M. Smirnov, Europhys. Lett. **97**, 33001 (2012).

17. L. D. Landau and E. M. Lifshitz, *Fluid Mechanics*, Butterworth, Oxford (2000).

18. B. M. Smirnov, *Nanoclusters and Microparticles in Gases and Vapors*, DeGruyter, Berlin (2012).

19. B. M. Smirnov, *Clusters and Small Particles in Gases and Plasmas*, Springer, New York (1999).

20. *Handbook of Chemistry and Physics*, edition 86, ed. by D. R. Lide, CRC Press, London (2003–2004).

21. B. M. Smirnov, *Cluster Processes in Gases and Plasmas*, Wiley, Berlin (2010).

22. E. P. Wigner and F. Seits, Phys. Rev. **46**, 509 (1934).

23. E. P. Wigner, Phys. Rev. **46**, 1002 (1934).

24. S. Ino, J. Phys. Soc. Jpn. **27**, 941 (1969).

25. L. D. Landau and E. M. Lifshitz, *Electrodynamics of Continuous Media*, Pergamon Press, Oxford (1984).

26. W. Wien, Wied. Ann. **58**, 662 (1896).

27. M. V. Smolukhowskii, Zs. Phys. **17**, 585 (1916).

28. B. M. Smirnov, *Reference Data on Atomic Physics and Atomic Processes*, Springer, Berlin (2008).

29. N. B. Vargaftik, *Tables of Thermophysical Properties of Liquids and Gases*, Halsted Press, New York (1975).

30. B. M. Smirnov, Plasma Chem. Plasma Proc. **13**, 673 (1993).

31. N. B. Vargaftic, L. N. Filipov, A. A. Tarismanov, and E. E. Totzkii, *Handbook for Thermal Conductivitity of Liquids and Gases*, CRC Press, Boca Raton (1994).

32. B. M. Smirnov, Uspekhi Fiz. Nauk **164**, 665 (1994).

33. P. Meakin, Phys. Rev. Lett. **51**, 1119 (1983).

34. R. Jullien and R. Botet, *Aggregation and Fractal Aggregates*, World Sci., Singapore (1987).

35. B. M. Smirnov, Phys. Rep. **188**, 1 (1990).

36. Y. Kantor and T. A. Witten, J. de Phys. **45**, L674 (1984).

37. A. A. Lushnikov, A. E. Negin, and A. V. Pakhomov, Chem. Phys. Lett. **175**, 138 (1990).

38. A. A. Lushnikov, A. E. Negin, A. V. Pakhomov, and B. M. Smirnov, Uspekhi Fiz. Nauk **161**(2), 113 (1991).

39. B. M. Smirnov, Uspekhi Fiz. Nauk **161**(8), 141 (1991).

40. *Aerogels*, ed. by J. Fricke, Springer, Berlin (1985).

41. *Aerogels*, ed. by J. Fricke, Springer, Berlin (1987).

42. P. C. Reist, *Introduction to Aerosol Science*, Macmillan Publ. Comp., New York (1984).

43. T. M. Peters, J. Volckens, and S. V. Hering, *Impactors, Cyclones, and Other Particle Collectors*, Amer. Conf. Governm. Industr. Hygienist., Washington (2009).